Biophysical Chemistry 25 (1986) 147–159
Elsevier

BPC 01098

NONEQUILIBRIUM VOLTAGE FLUCTUATIONS IN BIOLOGICAL MEMBRANES

II. VOLTAGE AND CURRENT NOISE GENERATED BY ION CARRIERS, CHANNELS AND ELECTROGENIC PUMPS

Peter SOLLEDER and Eckart FREHLAND

Fakultäten für Biologie und Physik, Universität Konstanz, Postfach 5560, D-7750 Konstanz, F.R.G.

Received 19th February 1986
Revised manuscript received 28th August 1986
Accepted 10th September 1986

Key words: Ion carrier; Ion channel; Electrogenic pump; Nonequilibrium voltage fluctuation

As applications of the general theoretical framework of charge transport in biological membranes and related voltage and current noise, a number of model calculations are presented for ion carriers, rigid channels, channels with conformational substates and electrogenic pumps. The results are discussed with special reference to the problem of threshold values for sensory transduction processes and their limitations by voltage fluctuations. Furthermore, starting from the special results of model calculations, an attempt is made to determine more general aspects of electric fluctuations generated by charge-transport processes in biological membranes: different frequency dependences of voltage and current noise, and dependence of noise intensities with increasing distance from the equilibrium state.

1. Introduction

In recent years most experiments on electric noise generated by ion transport in biological membranes have been concerned with the analysis of current noise under voltage-clamp conditions (ref. 1 and work cited therein). Hence, most of the theoretical work concerning membrane noise has also focussed on the analysis of current noise [1–3]. In a number of papers the current noise generated under equilibrium or nonequilibrium conditions has been treated for different transport mechanisms: hydrophobic ions, ionic carriers, rigid and nonrigid pores and electrogenic pumps. However, it could be shown that all these processes can be treated with a general theoretical approach to transport noise in discrete systems developed some years ago [4]. Furthermore, in a preceding paper [5] (hereafter referred to as I) we have presented a corresponding general approach to voltage noise. In addition, we believe that it is now more sensible to give a summarizing presentation of voltage noise generated by basic ion-transport mechanisms in one paper than to produce a redundant series of theoretical papers as applications of one general formalism.

Moreover, there are no essential differences in the formal mathematical treatment of different processes such as carriers, electrogenic pumps and pores with conformational substates though the transport mechanisms themselves are essentially different. Additionally to voltage noise the corresponding current noise is calculated.

Using the results of these numerical model calculations in the final discussion (section 6) an attempt is made to determine characteristic noise properties and differences between (a) the different transport processes and (b) current and voltage noise.

In special applications, because of the com-

paratively large number of parameters involved in the model calculations with rather complex effects on the noise, we wish to caution against overinterpretations of experimental results. On the other hand, we believe that our careful discussion may lead to a deeper understanding of electric noise generated by complex charge-transport processes in biological membranes.

The occurrence of voltage fluctuations may be important for the control of processes in biological membranes on the molecular level. For example, the fluctuations give rise to a limit in the sensitivity of such processes. In section 6.4 we shall discuss the results with special reference to the problem of threshold values for sensory transduction processes.

2. Ion carriers

2.1. Basic discrete model

One basic concept of transport through membranes is that of carrier-mediated ion transport. For example, valinomycin-mediated transport through lipid bilayer membranes has been extensively investigated (e.g. refs. 6–8). The experimental and theoretical analysis of carrier-generated current noise under equilibrium and nonequilibrium conditions has been performed some years ago [9]. Recently, experiments on carrier-mediated voltage noise have been described [10].

The mechanism as proposed 15 years ago [6,7] represents the minimum discrete model containing the essential properties of the carrier mechanism.

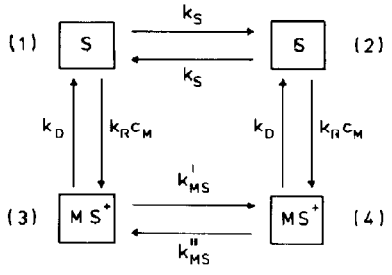

Fig. 1. State diagram for modelling carrier-mediated ion transport.

It is an important example, which shows the applicability and usefulness of the discrete transport concept. As shown in fig. 1 the four essential steps of the process are: (a) recombination of an ion M^+ and the neutral carrier S at one interface, (b) translocation of the charged complex to the other interface, (c) dissociation of the complex and (d) back transport of the free neutral carrier. Thus, the ion transport (step b) is coupled to chemical reaction processes (recombination a and dissociation c).

2.2. Kinetic equations, Fokker-Planck moments

In the case of carrier-mediated ion transport we will illustrate explicitly the derivation of the kinetic equations and Fokker-Planck moments (cf. I) under varying voltage conditions.

The total carrier concentration N_0 in the membrane is assumed to be constant:

$$N_0 = N'_S + N''_S + N'_{MS} + N''_{MS}, \tag{1}$$

where N'_S, N''_S, N'_{MS} and N''_{MS} are the interfacial concentrations at the left and right interface, respectively. The time-dependent behavior of the system under constant-voltage conditions (cf. eq. 8 in I) is given by the following equations [10]:

$$\begin{aligned}
\frac{d\langle N'_S\rangle}{dt} &= -k_R c_M \langle N'_S\rangle + k_D \langle N'_{MS}\rangle \\
&\quad - k_S(\langle N'_S\rangle - \langle N''_S\rangle) \\
\frac{d\langle N''_S\rangle}{dt} &= -k_R c_M \langle N''_S\rangle + k_D \langle N''_{MS}\rangle \\
&\quad - k_S(\langle N''_S\rangle - \langle N'_S\rangle) \\
\frac{d\langle N'_{MS}\rangle}{dt} &= k_R c_M \langle N'_S\rangle - k_D \langle N'_{MS}\rangle \\
&\quad - k'_{MS}\langle N'_{MS}\rangle + k''_{MS}\langle N''_{MS}\rangle \\
\frac{d\langle N''_{MS}\rangle}{dt} &= k_R c_M \langle N''_S\rangle - k_D \langle N''_{MS}\rangle \\
&\quad - k''_{MS}\langle N''_{MS}\rangle + k'_{MS}\langle N'_{MS}\rangle
\end{aligned} \tag{2}$$

k_R and k_D are the rate constants characterizing the association and dissociation, respectively. The translocation of the uncharged, charged carrier is described by the rate constants k_S and k'_{MS}, k''_{MS}, respectively.

In case the system is not kept under constant voltage the voltage itself has to be taken as a further variable (cf. I) and the voltage dependence of the rate constants has to be considered. Only the transitions $(3 \rightarrow 4)$ and $(4 \rightarrow 3)$ generate a change of voltage because they are connected with the transport of a charge. The voltage dependence of the rate constants k'_{MS} and k''_{MS} is given by (cf. eq. 14 in I):

$$k'_{MS} = k'_{MS}(V^S) \exp\left(\frac{q}{2k_B T}\Delta V\right)$$

$$k''_{MS} = k''_{MS}(V^S) \exp\left(-\frac{q}{2k_B T}\Delta V\right) \tag{3a}$$

with the linearization for small deviations ΔV from V^S:

$$k'_{MS} = k''_{MS}(V^S)\left(1 + \frac{q}{2k_B T}\Delta V\right)$$

$$k''_{MS} = k''_{MS}(V^S)\left(1 - \frac{q}{2k_B T}\Delta V\right) \tag{3b}$$

Introducing the deviations α_μ from the steady state N^S_μ we obtain from eq. 2 with eq. 3b the linearized equations

$$\frac{d\langle\alpha'_S\rangle}{dt} = -k_R c_M\langle\alpha'_S\rangle + k_D\langle\alpha'_{MS}\rangle - k_S(\langle\alpha'_S\rangle - \langle\alpha''_S\rangle)$$

$$\frac{d\langle\alpha''_S\rangle}{dt} = -k_R c_M\langle\alpha''_S\rangle + k_D\langle\alpha''_S\rangle - k_S(\langle\alpha''_S\rangle - \langle\alpha'_S\rangle)$$

$$\frac{d\langle\alpha'_{MS}\rangle}{dt} = k_R c_M\langle\alpha'_S\rangle - k_D\langle\alpha'_{MS}\rangle - \bar{k}'_{MS}\langle\alpha'_{MS}\rangle + \bar{k}''_{MS}\langle\alpha''_{MS}\rangle - \frac{q}{2k_B T}\phi\langle\Delta V\rangle$$

$$\frac{d\langle\alpha''_{MS}\rangle}{dt} = k_R c_M\langle\alpha''_S\rangle - k_D\langle\alpha''_{MS}\rangle - \bar{k}''_{MS}\langle\alpha''_{MS}\rangle + \bar{k}'_{MS}\langle\alpha'_{MS}\rangle + \frac{q}{2k_B T}\phi\langle\Delta V\rangle \tag{4}$$

with

$$\bar{k}'_{MS} = k'_{MS}(V^S)$$

$$\bar{k}''_{MS} = k''_{MS}(V^S)$$

and

$$\phi = \bar{k}'_{MS}N'^S_{MS} + \bar{k}''_{MS}N''^S_{MS}$$

The time-dependent behavior of ΔV under current-clamp is described by (cf. eq. 19b in I):

$$\frac{d\langle\Delta V\rangle}{dt} = -\frac{q}{C}\bar{k}'_{MS}\langle\alpha'_{MS}\rangle + \frac{q}{C}\bar{k}''_{MS}\langle\alpha''_{MS}\rangle - \frac{q^2}{2k_B TC}\phi\langle\Delta V\rangle \tag{5}$$

This linear system of equations (eqs. 4 and 5) describes the kinetic behavior of the carrier system under current-clamp for small ΔV and serves as a basis for calculating the voltage noise. For the further treatment we use the matrix notation (cf. I):

$$\frac{d\langle\boldsymbol{\beta}\rangle}{dt} = -\boldsymbol{K}\langle\boldsymbol{\beta}\rangle \tag{6}$$

with

$$\langle\beta_\mu\rangle = \langle\alpha_\mu\rangle \quad (\mu = 1,\ldots,4)$$

$$\langle\beta_5\rangle = \langle\Delta V\rangle$$

$\boldsymbol{K}$ follows from eqs. 4 and 5.

Furthermore, for determination of the spectral density of voltage fluctuations we need the Fokker-Planck moments, which according to eq. 38 in I in the case of carrier-mediated ion transport, are given by

$$\begin{aligned} B_{12} &= B_{21} = -k_S\left(N'^S_S + N''^S_S\right) \\ B_{13} &= B_{31} = -\left(k_R c_M N'^S_S + k_D N'^S_{MS}\right) \\ B_{24} &= B_{42} = -\left(k_R c_M N''^S_S + k_D N''^S_{MS}\right) \\ B_{34} &= B_{43} = -\phi \end{aligned} \tag{7}$$

The remaining elements can be derived from

$$B_{\mu\mu} = -\sum_{\substack{\nu=1 \\ \nu\neq\mu}}^{4} B_{\nu\mu} \quad (\mu = 1,\ldots,4) \tag{8}$$

and

$$B_{i5} = B_{5i} = \frac{2k_B T}{C}K_{i5} \quad (i = 1,\ldots,5)$$

2.3. Voltage and current noise generated by ion carriers

With eqs. 6–8 the spectral density of voltage fluctuations can be calculated as the (5,5) component of the spectral density matrix (cf. eq. 41 in I)

$$G_{\Delta V}(\omega) = 2\left[(\boldsymbol{K}^2 + \omega^2\boldsymbol{E})^{-1}\boldsymbol{K}\boldsymbol{B}\tilde{\boldsymbol{K}}(\tilde{\boldsymbol{K}}^2 + \omega^2\boldsymbol{E})^{-1} + \omega^2(\boldsymbol{K}^2 + \omega^2\boldsymbol{E})^{-1}\boldsymbol{B}(\tilde{\boldsymbol{K}}^2 + \omega^2\boldsymbol{E})^{-1}\right]_{5,5}$$

where $\tilde{\boldsymbol{K}}$ is the transposed matrix of $\boldsymbol{K}$ and $\boldsymbol{B}$ is the matrix of the Fokker-Planck moments. We derived two sets of equations (eqs. 2 and 6). The second one reduces to the first in the case where constant-voltage conditions are assumed.

The nonequilibrium current noise generated by ion carriers has been analyzed some years ago [7]. Using the rate constants as determined by Benz and Läuger [8] for valinomycin-mediated transport, we have calculated the expected voltage and current noise. The results are given in fig. 2. The voltage noise exhibits Lorentzian behavior with increasing low-frequency intensity for increasing voltage, while the current noise shows inverse Lorentzian behavior which is typical for transport noise (cf. ref. 9 and the discussion in section 6.2). For both types of noise at nonequilibrium (100 mV) the Nyquist relation is not valid. The corresponding contributions from the admittance $Y(\omega)$ as expected from the Nyquist relations (eqs. 45 and 46 in I) are drawn in fig. 2a and b.

3. Rigid pores

3.1. Discrete modelling of ion transport through rigid pores

A rigid pore denotes a hydrophilic pathway through a membrane which is seen by the ion as a fixed structure not changing in time. If the hydrophilic pathway can be regarded as a discrete sequence of ionic binding sites the transports is a jump-diffusion process which can be described by discrete models [11–13]. For the case of vanishing interactions between the ions, the discrete jump-diffusion pore models [14] are mathematically equivalent to the so-called compartment models [15,16]. 30 years ago the single-file mechanism for ionic transport through narrow pores was proposed by Hodgkin and Keynes [17] in order to explain anomalous flux ratio exponents of Ussing's criterion [18]. The basic idea of single-file diffusion consists of constraining the movement of the ions to one dimension and of not allowing the ions to overtake each other. Recently, the concept of time-dependent transport through rigid pores has been extensively studied in a series of papers

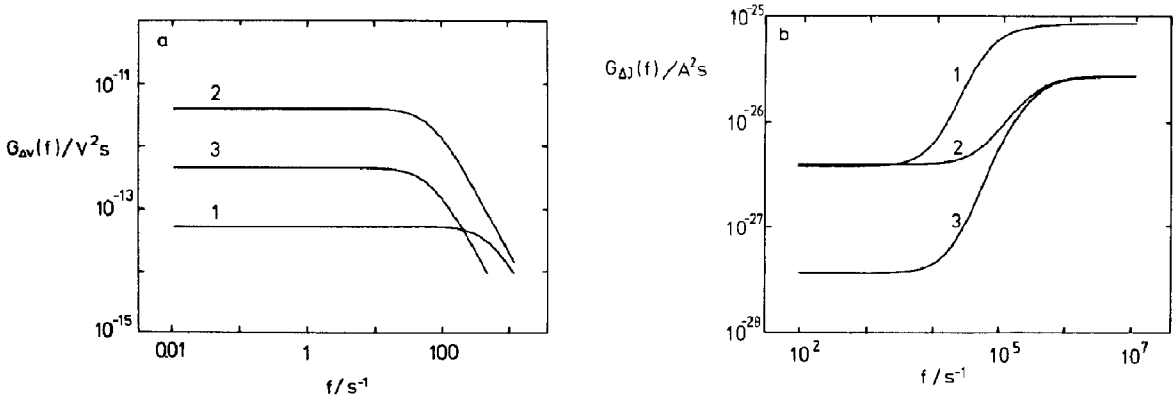

Fig. 2. (a) Voltage noise for carrier-mediated ion transport at equilibrium (1) and nonequilibrium $V = 100$ mV (2). $4kTRe(1/Y)$ (3). Parameters: $k_R = 2.9\times10^5$ M^{-1} s^{-1}, $k_D = 2.7\times10^5$ s^{-1}, k_{MS} $(V=0) = 2.1\times10^5$ s^{-1}, $k_S = 3.8\times10^4$ s^{-1}, $C_m = 1$ μF/cm^2, $A = 10^4$ μm^2, $N_0/A = 10^3$ μm^{-2}, $c_M = 1$ M. (b) Current noise for carrier-mediated ion transport at equilibrium (1) and nonequilibrium, $V = 100$ mV (2). $4kTRe(Y)$ (3). Parameters as in panel a.

[14,20,21]. The essential point in the discrete modelling of single-file transport is the description in terms of the ionic occupation states of the pores.

In fig. 3 the discrete graphs for the one- and two-site pores are shown. Using these graphs the kinetic equations are formulated in the following.

3.2. Kinetic equations for pores with one and two binding sites

3.2.1. One binding site

We will first consider the case of pores with only one binding site. The rate constants describing the jumps from and to this binding site are

$$K_1 = k' + k''$$
$$K_2 = k_1 + k_r \tag{9}$$

N_1 and N_2 denote the numbers of occupied and unoccupied pores, respectively. The total number N_0 of pores is assumed to be constant:

$$N_0 = N_1 + N_2 \tag{10}$$

The linearized kinetic equations for the time-dependent behavior under current-clamp conditions for small deviations V from V^S are

$$\frac{d\langle\alpha_1\rangle}{dt} = -\bar{K}_1\langle\alpha_1\rangle + \bar{K}_2\langle\alpha_2\rangle + \frac{1}{2k_BT}(\gamma_1\phi_1 - \gamma_2\phi_2)\langle\Delta V\rangle$$

$$\frac{d\langle\alpha_2\rangle}{dt} = \bar{K}_1\langle\alpha_1\rangle - \bar{K}_2\langle\alpha_2\rangle - \frac{1}{2k_BT}(\gamma_1\phi_1 - \gamma_2\phi_2)\langle\Delta V\rangle$$

$$\frac{d\langle\Delta V\rangle}{dt} = \frac{1}{C}(\gamma_1\bar{k}'' - \gamma_2\bar{k}')\langle\alpha_1\rangle - \frac{1}{C}(\gamma_1\bar{k}_1 - \gamma_2\bar{k}_r)\langle\alpha_2\rangle - \frac{1}{2k_BTC}(\gamma_1^2\phi_1 + \gamma_2^2\phi_2)\langle\Delta V\rangle \tag{11}$$

with

$$\phi_1 = \bar{k}_1 N_2^S + \bar{k}'' N_1^S$$
$$\phi_2 = \bar{k}_r N_2^S + \bar{k}'' N_1^S$$
$$\bar{k}_i = k_i(V^S).$$

γ_1 and γ_2, respectively, are defined in eq. 11 of I, with

$$\gamma_1 + \gamma_2 = q$$

Under voltage-clamp conditions eqs. 11 reduce to

$$\frac{d\langle\alpha_1\rangle}{dt} = -\bar{K}_1\langle\alpha_1\rangle + \bar{K}_2\langle\alpha_2\rangle$$
$$\frac{d\langle\alpha_2\rangle}{dt} = \bar{K}_1\langle\alpha_1\rangle - \bar{K}_2\langle\alpha_2\rangle \tag{12}$$

The Fokker-Planck moments are:

$$B_{11} = B_{22} = \bar{K}_1 N_1^S + \bar{K}_2 N_2^S$$
$$B_{12} = B_{21} = -(\bar{K}_1 N_1^S + \bar{K}_2 N_2^S)$$
$$B_{13} = B_{31} = -B_{23} = -B_{32} = -\frac{1}{C}(\gamma_1\phi_1 - \gamma_2\phi_2)$$
$$B_{33} = \frac{1}{C^2}(\gamma_1^2\phi_1 + \gamma_2^2\phi_2) \tag{13}$$

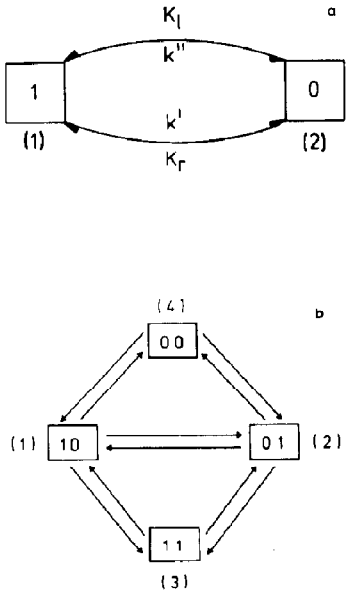

Fig. 3. State diagrams for single-file transport of one ion species through rigid pores with one (a) and two (b) binding sites.

3.2.2. Two binding sites

The matrix of coefficients K for a pore with

two binding sites is given by

$$K_{ij} = -\bar{k}_{ij} \quad (i \neq j)$$

$$K_{jj} = \sum_{\substack{i=1 \\ i \neq j}}^{4} \bar{k}_{ij} \quad (j = 1, \ldots, 4) \tag{14}$$

where the rate constants $\bar{k}_{ij}$ denote transitions $(j \to i)$ at voltage V^S. The remaining elements are

$$K_{15} = -\frac{1}{2k_BT}(\gamma_1\phi_{1a} + \gamma_3\phi_{3a} - \gamma_2\phi_2)$$

$$K_{25} = -\frac{1}{2k_BT}(\gamma_2\phi_2 - \gamma_1\phi_{1b} - \gamma_3\phi_{3b})$$

$$K_{35} = -\frac{1}{2k_BT}(\gamma_1\phi_{1b} - \gamma_3\phi_{3a})$$

$$K_{45} = -\frac{1}{2k_BT}(\gamma_3\phi_{3b} - \gamma_1\phi_{1a})$$

$$K_{55} = \frac{1}{2k_BTC}\left(\gamma_1^2(\phi_{1a} + \phi_{1b}) + \gamma_2^2\phi_2 + \gamma_3^2(\phi_{3a} + \phi_{3b})\right)$$

$$K_{51} = \frac{1}{C}(\gamma_2\bar{k}_{21} - \gamma_3\bar{k}_{31} - \gamma_1\bar{k}_{41})$$

$$K_{52} = \frac{1}{C}(\gamma_3\bar{k}_{42} - \gamma_2\bar{k}_{12} - \gamma_1\bar{k}_{32})$$

$$K_{53} = \frac{1}{C}(\gamma_3\bar{k}_{13} - \gamma_1\bar{k}_{23})$$

$$K_{54} = \frac{1}{C}(\gamma_1\bar{k}_{14} - \gamma_3\bar{k}_{24}) \tag{15}$$

In eq. 15 the following definitions for the stationary fluxes are used

$$\phi_{1a} = \bar{k}_{14}N_4^S + \bar{k}_{41}N_1^S$$
$$\phi_{1b} = \bar{k}_{23}N_3^S + \bar{k}_{32}N_2^S$$
$$\phi_2 = \bar{k}_{12}N_2^S + \bar{k}_{21}N_1^S$$
$$\phi_{3a} = \bar{k}_{13}N_3^S + \bar{k}_{31}N_1^S$$
$$\phi_{3b} = \bar{k}_{24}N_4^S + \bar{k}_{42}N_2^S \tag{16}$$

With eqs. 16 we are able to write down the Fokker-Planck moments:

$$B_{12} = B_{21} = -\phi_2$$
$$B_{13} = B_{31} = -\phi_{3a};\ B_{14} = B_{41} = -\phi_{1a}$$
$$B_{24} = B_{42} = -\phi_{3b};\ B_{23} = B_{32} = -\phi_{1b} \tag{17a}$$

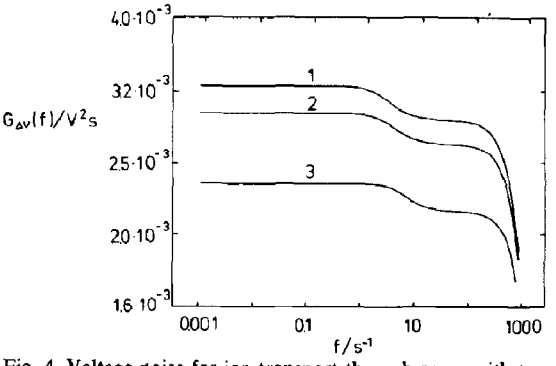

Fig. 4. Voltage noise for ion transport through pores with two binding sites at different voltages: (1) $u = 0$, (2) $u = 2.5$ and (3) $u = 5$, with the reduced voltage $u = qV/k_BT$. Parameters: $\gamma_1 = \gamma_2 = \gamma_3 = 1/3$ q; $N_0 = 10^4$, $C = 1$ F, $k(0) = 1$; q: charge of one ion.

and

$$B_{\mu\mu} = -\sum_{\substack{\nu=1 \\ \nu \neq \mu}}^{4} B_{\nu\mu} \quad (\mu = 1, \ldots, 5)$$

$$B_{5i} = B_{i5} = \frac{2k_BT}{C}K_{i5} \quad (i = 1, \ldots, 5) \tag{17b}$$

3.3. *Voltage noise*

The voltage noise generated by rigid pores with one binding site has been analysed in a recent paper [22] with a slightly different approach, where instead of voltage the difference between charge density on the membrane surfaces is used. The agreement between the two approaches can be explicitly shown.

A numerical example of voltage noise generated by a system of rigid two-binding-site pores, calculated with the use of eqs. 14–17 and the general voltage-noise formula (eq. 41 in I), is presented in fig. 4. As for the rigid one-binding-site pores the low-frequency noise decreases with increasing voltage (cf. the discussion of this point in section 6.2).

4. Channels with different conformational states

4.1. *Modelling of channels with fluctuating structures*

Recent studies of protein dynamics show that proteins may assume a number of conformational

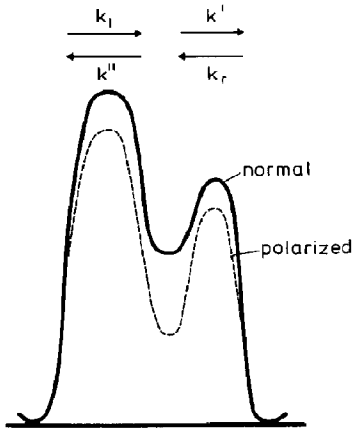

Fig. 5. Energy profile of a channel with one binding site in the 'normal' and 'polarized' state. k', k', k_l and k_r are the rate constants for transfer of an ion between binding site and external solution in the normal state.

states [23,24] (fig. 5). The transitions between different states may occur in the time range from picoseconds to seconds. Different substates may exhibit different ionic conductances. The potential profiles for the example of a one-binding-site channel with a 'normal' and a 'polarized' substate are given in fig. 5.

The special situation of channel kinetics may be modelled under the assumption that at least one state has vanishing conductance (open-closed kinetics).

Though the situation is more complex than in the case of rigid single file pores, the discrete description may generally be used by the introduction of additional states [5,25–27]. In fig. 6a and b the state diagrams are shown for channel models with one ionic binding site and two conformational states. In fig. 6a both states have nonvanishing conductance: in fig. 6b one state has vanishing conductance. In the latter case it is assumed that the conformational transitions strongly depend on the ionic occupation state: the transition probability into the closed state is set at zero for the occupied channel. This assumption seems reasonable because of experimental findings that the lifetimes of open nerve channels increase with increasing ionic concentrations [28]. The corresponding finding for apical amiloride-blocked sodium-selective channels has recently been modelled and theoretically analyzed in an analogous way by the assumption of competition between amiloride and sodium [29].

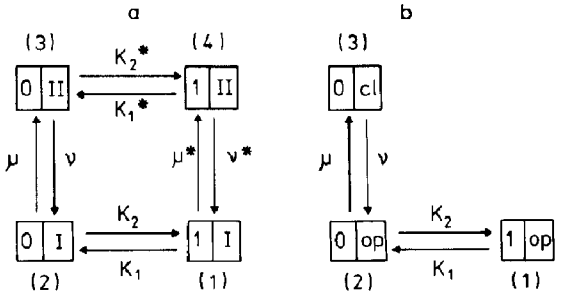

Fig. 6. State diagrams for channels with one binding site and two conducting states (a) or with open-closed kinetics (b). μ, ν, μ^* and ν^* describe the transitions between the different conducting states.

The following model calculations concentrate on the case shown in fig. 6b.

4.2. Kinetic equations, Fokker-Planck moments

We will first give the kinetic equations for channels with open-closed kinetics (cf. fig. 6b). We distinguish between rate constants μ, ν for open-closed transitions. Transitions between the open-unoccupied and open-occupied states are determined by jumps of ions from and to the left- and right-hand sides of the channel, respectively. Therefore, according to fig. 6b

$$K_1 = k' + k''$$
$$K_2 = k_l + k_r \tag{18}$$

The rate constants μ and ν are assumed to be independent of voltage. The time-dependent behavior is given by

$$\frac{\mathrm{d}\langle \boldsymbol{\beta} \rangle}{\mathrm{d}t} = -\boldsymbol{K}\langle \boldsymbol{\beta} \rangle \tag{19}$$

where

$$\langle \beta_\mu \rangle = \langle N_\mu \rangle - N_\mu^S \quad (\mu = 1, \ldots, 3)$$
$$\langle \beta_4 \rangle = \langle \Delta V \rangle$$

and the matrix of coefficients has the elements

$$K = \begin{bmatrix} \bar{K}_1 & -\bar{K}_2 & 0 & -\frac{1}{2k_BT}(\gamma_1\phi_1 - \gamma_2\phi_2) \\ -\bar{K}_1 & \bar{K}_2 + \mu & -\nu & \frac{1}{2k_BT}(\gamma_1\phi_1 - \gamma_2\phi_2) \\ 0 & -\mu & \nu & 0 \\ -\frac{1}{C}(\gamma_1\bar{k}'' - \gamma_2\bar{k}') & \frac{1}{C}(\gamma_1\bar{k}_1 - \gamma_2\bar{k}_r) & 0 & -\frac{1}{2k_BTC}(\gamma_1^2\phi_1 - \gamma_2^2\phi_2) \end{bmatrix} \tag{20}$$

ϕ_1 and ϕ_2 are defined correspondingly as in eq. 11 with N_1^S and N_2^S as stationary solutions of eq. 19. The Fokker-Planck moments are

$$\begin{aligned} B_{11} &= \bar{K}_1 N_1^S + \bar{K}_2 N_2^S \\ B_{21} &= B_{12} = -B_{11} \\ B_{13} &= B_{31} = B_{34} = B_{43} = 0 \\ B_{14} &= B_{41} = -B_{24} = -B_{42} = -\frac{1}{C}(\gamma_1\phi_1 - \gamma_2\phi_2) \\ B_{22} &= B_{11} + \mu N_2^S + \nu N_3^S \\ B_{23} &= B_{32} = -(\mu N_2^S + \nu N_3^S) \\ B_{33} &= -B_{23} \\ B_{44} &= \frac{1}{C^2}(\gamma_1^2\phi_1 - \gamma_2^2\phi_2) \end{aligned} \tag{21}$$

The transitions $(2 \to 3)$ and $(3 \to 2)$, respectively, do not contribute to the Fokker-Planck moments $B_{j4} = B_{4j}$ $(j = 1, \ldots, 4)$ because they are voltage-independent.

The set of equations (eq. 19) can be easily extended to channels with two conducting substates (fig. 7a). We obtain

$$\frac{d\langle\beta\rangle}{dt} = -K\langle\beta\rangle$$

with

$$\langle\beta_\mu\rangle = \langle N_\mu\rangle - N_\mu^S \quad (\mu = 1, \ldots, 4)$$

and

$$\langle\beta_5\rangle = \langle\Delta V\rangle$$

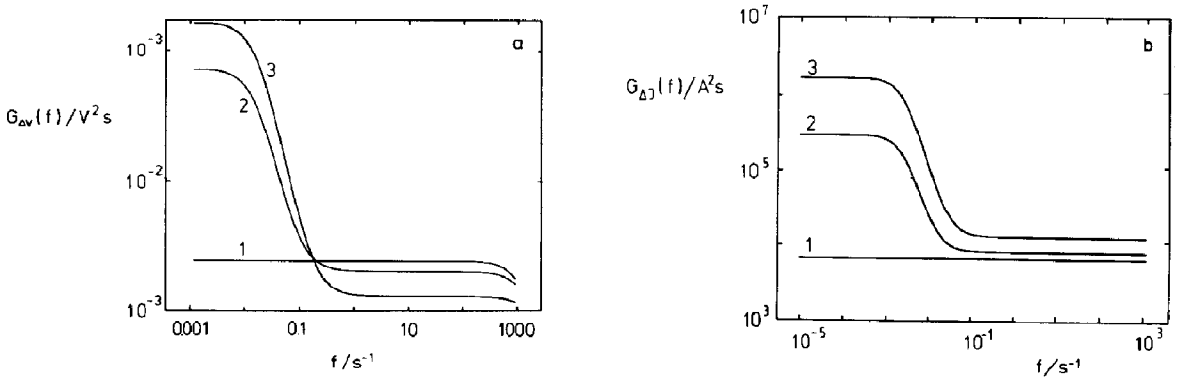

Fig. 7. (a) Voltage noise for a transport system of channels with open-closed kinetics at different voltages: (1) $u = 0$, (2) $u = 2.5$, (3) $u = 5$, with $u = qV/k_BT$. Parameter: $k_1(0) = k_r(0) = k'(0) = k''(0) = 1$; $\nu = \mu = 0.01$; $C = 1$ F; $N_0 = 10^4$; $\gamma_1 = \gamma_2 = 1/2$. (b) Current noise of a transport system of channels with one binding site and open-closed kinetics at different voltages. Parameters and voltages as in panel a.

$\boldsymbol{K}$ is given by

$$\boldsymbol{K} = \begin{bmatrix} \bar{K}_1 + \mu^* & -\bar{K}_2 & 0 & -\nu^* & -\frac{1}{2k_BT}(\gamma_1\phi_1 - \gamma_2\phi_2) \\ -\bar{K}_1 & \bar{K}_2 + \mu & -\nu & 0 & \frac{1}{2k_BT}(\gamma_1\phi_1 - \gamma_2\phi_2) \\ 0 & -\mu & \bar{K}_2^* + \nu & -\bar{K}_1^* & \frac{1}{2k_BT}(\gamma_1\phi_1^* - \gamma_2\phi_2^*) \\ -\mu^* & 0 & -\bar{K}_2^* & \bar{K}_1^* + \nu^* & -\frac{1}{2k_BT}(\gamma_1\phi_1^* - \gamma_2\phi_2^*) \\ -\delta_1 & \delta_2 & \delta_2^* & -\delta_1^* & \frac{1}{2k_BTC}(\gamma_1^2[\phi_1 + \phi_1^*] + \gamma_2^2[\phi_2 + \phi_2^*]) \end{bmatrix} \quad (22)$$

where we have used the abbreviations

$$\begin{aligned} \phi_1^* &= \bar{k}_1^* N_3^S + \bar{k}''^* N_4^S \\ \phi_2^* &= \bar{k}_r^* N_3^S + \bar{k}'^* N_4^S \\ \delta_1 &= \gamma_1\bar{k}'' - \gamma_2\bar{k}'; \quad \delta_1^* = \gamma_1\bar{k}''^* - \gamma_2\bar{k}'^* \\ \delta_2 &= \gamma_1\bar{k}_1 - \gamma_2\bar{k}_r; \quad \delta_2^* = \gamma_1\bar{k}_1^* - \gamma_2\bar{k}_r^* \end{aligned} \quad (23)$$

and ϕ_1 and ϕ_2 as in eq. 11.

For the Fokker-Planck moments hold the relations:

$$\begin{aligned} B_{12} &= B_{21} = -(\bar{K}_1 N_1^S + \bar{K}_2 N_2^S) \\ B_{14} &= B_{41} = -(\mu^* N_1^S + \nu^* N_4^S) \\ B_{23} &= B_{32} = -(\mu N_2^S + \nu N_3^S) \\ B_{34} &= B_{43} = -(\bar{K}_1^* N_4^S + \bar{K}_2^* N_3^S) \end{aligned} \quad (24)$$

and

$$B_{13} = B_{31} = B_{24} = B_{42} = 0$$

The remaining elements are given by

$$B_{\mu\mu} = -\sum_{\substack{\nu=1 \\ \nu\neq\mu}}^{4} B_{\nu\mu} \quad (\mu = 1, \ldots, 4) \quad (25)$$

and

$$B_{5i} = B_{i5} = \frac{2k_BT}{C} K_{i5} \quad (i = 1, \ldots, 5)$$

The rate constants ν, μ and ν^*, μ^* are voltage-independent. Therefore, they do not contribute to the Fokker-Planck moments $B_{i5} = B_{5i}$ $(i = 1, \ldots, 5)$.

4.3. Voltage and current noise

With eqs. 18–25 the calculation of voltage (and current) noise can be done as an application of the general approach. The numerical results presented in fig. 7 are concerned with the noise generated by channels with open-closed kinetics. The behavior of voltage and current noise as a function of frequency and applied voltage is similar (cf. discussion in section 6).

5. Electrogenic pumps

The modelling of active transport may also be based on the concept of discrete systems. Furthermore, the formal treatment is very similar to that for ion transport by carriers or through channels

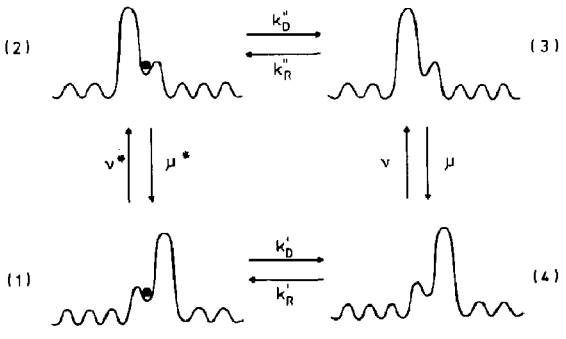

Fig. 8. State diagram for the most simple modelling of an electrogenic ion pump.

with different conformational substates. For example, the model situation of an ionic channel with two conformational states (fig. 6a) may be used as a minimum model of an ion pump if the energy profile is transiently modified in an appropriate way by an energy-supplying reaction [30,31] (cf. fig. 8).

5.1. Kinetic equations, Fokker-Planck moments

The time-dependent behavior of a transport system containing electrogenic ion pumps can be written in the following form

$$\frac{\mathrm{d}\langle\boldsymbol{\beta}\rangle}{\mathrm{d}t} = -\boldsymbol{K}\langle\boldsymbol{\beta}\rangle \tag{26}$$

with

$$\boldsymbol{K} = \begin{bmatrix} (\nu^* + k'_D) & -\mu^* & 0 & -k''_D & -\frac{q}{2k_BT}\phi \\ -\nu^* & (\mu^* + k'_R) & -k''_R & 0 & \frac{q}{2k_BT}\phi \\ 0 & -k'_R & (\mu + k''_R) & -\nu & 0 \\ -k'_D & 0 & -\mu & (\nu + k''_D) & 0 \\ \frac{q}{C}\nu^* & -\frac{q}{C}\mu^* & 0 & 0 & \frac{q^2}{2k_BTC}\phi \end{bmatrix} \tag{27}$$

where

$$\phi = \nu^* N_1^S + \mu^* N_2^S$$

The Fokker-Planck moments are:

$$B_{12} = B_{21} = -\left(\nu^* N_1^S + \mu^* N_2^S\right)$$

$$B_{14} = B_{41} = -\left(k'_D N_1^S + k'_R N_4^S\right)$$

$$B_{23} = B_{32} = -\left(k''_D N_2^S + k''_R N_3^S\right)$$

$$B_{34} = B_{43} = -\left(\mu N_3^S + \nu N_4^S\right) \tag{28}$$

The other elements of the Fokker-Planck matrix can be determined as described in eq. 25. One can define an equivalent voltage V_p (cf. ref. 32) to show the dependence of the rate constant ν^* on the driving force. We obtain

$$\nu^* = \frac{k'_D k''_R \mu^* \nu}{k''_D k'_R \mu} \exp(F \cdot V_P / R \cdot T) \tag{29}$$

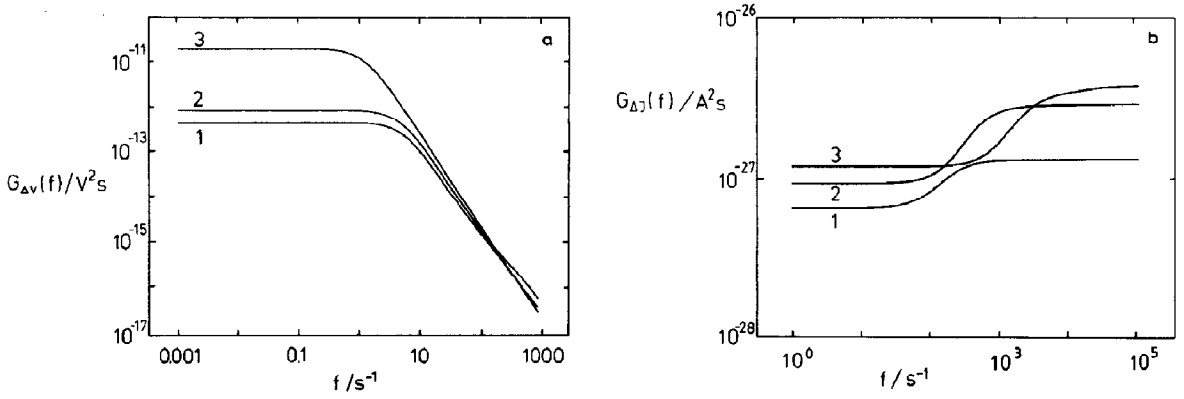

Fig. 9. (a) Voltage noise of an ion pump at different equivalent voltages: (1) $V_P = 0$ mV, (2) $V_P = 50$ mV, (3) $V_P = 100$ mV. Parameters: $k'_R = k'_D = k''_R = k''_D = 5 \times 10^4$ s^{-1}; $\nu^* = \mu^* = \nu = \mu = 500$ s^{-1}; $C_m = 1$ μF/cm^2; $A = 10^5$ μm^2; $N_P/A = 10^3$ μm^{-2}. (b) Current noise of an electrogenic ion pump at different voltages. Parameter and voltages as in panel a.

where

$$V_p = (\Delta\tilde{\mu} - \Delta G)/F$$

F is the Faraday constant and $\Delta\tilde{\mu}$ the electrochemical potential difference of the transported ion. ΔG is the Gibbs free energy of ATP hydrolysis.

5.2. Voltage and current noise

From the mathematical point of view the treatment of active transport raises no additional formal difficulties. The state diagram in fig. 8 is similar to the corresponding ones in figs. 1 and 6a for carrier-mediated transport and passive transport through channels with fluctuating barriers, respectively. The shape of the noise spectra strongly depends on the model parameters. The parameters chosen for the numerical calculations presented in fig. 9 are taken from realistic assumptions (cf. ref. 32). The qualitative behavior and the differences between voltage and current noise are similar as in the examples for carrier noise given in fig. 2.

6. Discussion

6.1. Dependence of noise properties on the variation of parameters and modification of models

We have restricted our calculations to the presentation of some selected model situations thus illustrating the general procedure of calculating the voltage noise generated by ion-transport processes which can be described by discrete models.

The general remarks, which have been made in the discussion of I, have been confirmed by these model calculations, e.g., the low-frequency voltage-noise intensity $G_{\Delta V}(\omega \to 0)$ decreases in inverse proportion to the number of transport units involved in the process, whereas on the other hand the high-frequency noise intensity increases. As a consequence the variance of fluctuations does not change dramatically. Indeed, and this seems to be a finding which is generally valid, the variance of voltage fluctuations at equilibrium as well as at nonequilibrium states does not essentially deviate from the equilibrium value $k_B T/C$ (cf. section 4.2 in I). In contrast to this finding the current-noise intensity is proportional to the number of (independently acting) transport units.

Generally, as we have demonstrated some years ago with an extensive study on current noise generated by rigid pores [13], the explicit dependence of noise on the model parameters of the transport system may be very complex and we again wish to caution against overinterpretation and the drawing of too specific conclusions from noise results on model parameters.

Nevertheless, we shall now try to ascertain aspects which can be understood from a more general point of view than the special choice of model parameters and thus can contribute to a deeper understanding of electric noise generated by charge transport in biological membranes.

6.2. Lorentzian vs. inverse Lorentzian behavior

Regarding the presented numerical results, there are two models, where the frequency dependences of voltage and current noise are significantly different: the carrier model (figs. 1 and 2) and the electrogenic pump model (figs. 8 and 9). In these cases the voltage-noise spectral density exhibits a typical Lorentzian behavior, decreasing with increasing frequency while current noise shows inverse Lorentzian behavior, i.e., increasing with increasing frequency. In earlier papers [4,13,25], we have explained the inverse Lorentzian as a typical outcome of the vectorial character of current: a stochastic fluctuation of current is preferably responded to by a current in the opposite direction, thus exhibiting a negative contribution to the autocorrelation function of current. Translated into the spectral density (frequency domain) by Fourier transformation (Wiener-Khintchine relation) this yields an inverse Lorentzian.

On the other hand, the voltage is formally treated in the linearized kinetic equations in the same way as the other scalar variables (occupation numbers, densities). As a consequence the voltage fluctuations behave similarly to scalar density fluctuations: a stochastic voltage fluctuation is responded to by a relaxation with preferably the

same sign. Translated into the spectral density behavior this yields the typical Lorentzian (cf. figs. 2a and 9a).

Naturally, there are situations where the current noise also shows a Lorentzian behavior. Such an example is given in fig. 7 by channel noise: the (scalar) fluctuations of the channels between different states of conductance modulate the electric current and thus favor a Lorentzian behavior of current noise (cf. also the extensive discussion of these transport models in ref. 25). In the case where the channel state kinetics are slow compared with the transport kinetics (ionic movement), which is a realistic situation, e.g., for ionic channels in nerve membranes, the observed current noise for low frequencies is pure Lorentzian and qualitatively resembles voltage noise.

6.3. Voltage dependence

As a further result the numerical model calculations show that there may be completely different dependences of noise intensity with growing distance from equilibrium (increasing mean voltage or current). On the one hand, because with increasing external force (voltage) the ionic movement is forced in one preferred direction, e.g., for ionic movement through rigid narrow pores, this may lead to an ordering of the processes with the consequence that the fluctuations decrease. For the chosen parameters this effect is observed in fig. 4. The ordering effect of single-file transport interactions far from equilibrium has already been discussed [34].

On the other hand, especially in situations where more or less voltage-independent reaction steps are involved in the transport models modulating the electric process, the amplitude of electric fluctuations may increase with increasing distance from equilibrium yielding an increasing noise intensity. This effect is particularly clear in the case of channel noise but can also be seen (for the chosen sets of model parameters) in the carrier and electrogenic pump calculations.

Obviously the voltage behavior of noise intensities is rather complex and strongly dependent on the model parameters. However, we believe that our interpretation of the effects in special models may also be used for interpretation of other situations.

6.4. Threshold values for sensory transduction processes

The voltage-noise amplitude represents a fundamental barrier for safe signal detection in voltage-controlled sensory transduction processes. According to Fain et al. [33] the threshold values for synaptic transmission and generation of action potentials by vertebrate photoreceptors are less than 10^{-5} V. According to our results the variance of voltage noise is approx. $k_B T/C$. For specific membrane capacitance $C_M \approx 1\ \mu F/cm^2$ and cell areas of approx. 10^2–$10^3\ \mu m^2$ a mean fluctuation $\sqrt{\sigma^2_{\Delta V}} \approx 10^{-4}$ V can be calculated. On the other hand, an effective variance may be defined by

$$\sigma^2_{eff} = \int_0^{f_c} G_{\Delta V}(f)\, df \tag{30}$$

where f_c is given by the characteristic time T_c for the sensory transduction process. Only the slow fluctuations of voltage below f_c can influence the sensory transduction. According to our results the low-frequency voltage decreases with increasing number of transport units and the noise is shifted to high-frequency fluctuations which do not disturb sensory transduction. Thus, from the viewpoint of safe signal detection, a sufficient number of transport units seems to be favorable.

Acknowledgement

This article contains essential parts of P.S.'s Ph.D. thesis, 'Theoretische Untersuchungen elektrischer Fluktuationen in biologischen Membranen' (Konstanz, 1985).

References

1 L.J. De Felice, Introduction to membrane noise (Plenum Press, New York, 1981).
2 E. Frehland, Biophys. Chem. 8 (1978) 255.
3 Y.-D. Chen, Adv. Chem. Phys. 37 (1978) 67.
4 E. Frehland, Stochastic transport processes in discrete biological systems (Springer-Verlag, Berlin, 1982).

5 E. Frehland and P. Solleder, Biophys. Chem. 25 (1986) 135.
6 P. Läuger and G. Stark, Biochim. Biophys. Acta 211 (1970) 458.
7 G. Stark, B. Ketterer, R. Benz and P. Läuger, Biophys. J. 11 (1971) 981.
8 R. Benz and P. Läuger, J. Membrane Biol. 27 (1976) 171.
9 H.-A. Kolb and E. Frehland, Biophys. Chem. 12 (1980) 21.
10 S.M. Bezrukov, G.M. Drabkin, L.A. Fanina, A.I. Irkhin, E.I. Melnik and A.I. Sibilev, Acad. Sci. U.S.S.R, Leningrad Nucl. Phys. Inst. 598 (1980) p. 36.
11 P. Läuger, Biochim. Biophys. Acta 311 (1973) 423.
12 E. Frehland and P. Läuger, J. Theor. Biol. 47 (1974) 189.
13 E. Frehland and K.H. Faulhaber, Biophys. Struct. Mech. 7 (1980) 1.
14 E. Frehland and W. Stephan, J. Theor. Biol. 103 (1983) 77.
15 J.F. Danielli, J. Physiol. 96 (1939) 2.
16 H. Eyring, R. Lumry and J.W. Woodbury, Rec. Chem. Prog. 10 (1949) 100.
17 A.L. Hodgkin and R.D. Keynes, J. Physiol. 128 (1955) 61.
18 H.H. Ussing, Acta Physiol. Scand. 19 (1949) 43.
19 K. Heckmann, Biomembranes 3 (1972) 127.
20 W. Stephan and E. Frehland, J. Theor. Biol. 103 (1983) 481.
21 W. Stephan, B. Kleutsch and E. Frehland, J. Theor. Biol. 105 (1983) 287.
22 E. Frehland and P. Solleder, Eur. Biophys. J. 11 (1985) 167.
23 H. Frauenfelder, G.A. Petsko and D. Tsernoglu, Nature 280 (1979) 558.
24 M. Karplus and J.A. McCammon, Annu. Rev. Biochem. 52 (1983) 263.
25 E. Frehland, Biophys. Struct. Mech. 5 (1979) 91.
26 P. Läuger, W. Stephan and E. Frehland, Biochim. Biophys. Acta 602 (1980) 167.
27 P. Läuger, Biophys. J. 47 (1985) 581.
28 W. Stühmer and F. Conti, in: Annual Meeting of the Deutsche Gesellschaft für Biophysik, eds., G. Adam and G. Stark (Springer, Berlin, 1979) p. 84.
29 E. Frehland, T. Hoshiko and S. Machlup, Biochim. Biophys. Acta 732 (1983) 636.
30 C.S. Patlak, Bull. Math. Biophys. 19 (1956) 209.
31 P. Läuger, Biochim. Biophys. Acta 553 (1979) 143.
32 P. Läuger, Eur. Biophys. J. 11 (1984) 117.
33 G.L. Fain, A.M. Granda and J.H. Maxwell, Nature 265 (1977) 181.
34 E. Frehland, Synergetics – From microscopic to macroscopic order (Springer, Berlin, 1984)